

3/2 harmonic generation by femtosecond laser pulses in steep-gradient plasmas

A. Tarasevitch,* C. Dietrich, C. Blome, K. Sokolowski-Tinten, and D. von der Linde

Institut für Laser-und Plasmaphysik, Universität Essen-Duisburg, D-45117 Essen, Germany

(Received 30 December 2002; revised manuscript received 12 May 2003; published 20 August 2003)

The onset of an electron parametric instability and 3/2 harmonic generation in variable-scale-length plasmas on solid surfaces using femtosecond pulses is observed. With the intensity approaching 10^{18} W/cm², the instability threshold is already reached at plasma scale lengths of the order of the laser wavelength. A well-collimated harmonic emission with unusually broad spectrum is obtained.

DOI: 10.1103/PhysRevE.68.026410

PACS number(s): 52.38.Dx, 42.65.Ky, 52.35.Mw, 52.50.Jm

I. INTRODUCTION

The development of high-power femtosecond lasers has made it possible to carry out experiments on laser-plasma interactions in the relativistic regime. Experiments at this intensity level are of great interest because they can provide useful information for a number of applications such as fast ignition of laser fusion targets [1], particle acceleration [2], hard x ray [2], and high order harmonic generation [3]. Plasma parametric instabilities can play an important role in these applications. Important is that completely new regimes of plasma instabilities, not evident at lower intensities, can be expected. For example, a merging of different types of instabilities and a widening of the instability regions in \mathbf{k} space [4,5] can occur.

The laser plasma generated by femtosecond pulses on solid surfaces is strongly inhomogeneous. The gradient scale length L can be shorter than the laser wavelength λ_0 , $L \lesssim \lambda_0$. Both theoretical and experimental data on the instability development in such plasmas are lacking. The existing models deal mostly with relatively long spatial and temporal scales and with moderate intensities that are typical of nano and subnanosecond laser plasma interactions [6,7]. Also, in the models that take relativistic effects into account, it is supposed either that the plasma is homogeneous, or that $L/\lambda_0 \gg 1$ [4,5].

A serious experimental difficulty in high intensity femtosecond laser solid interactions is that the plasma scale length is very difficult to control. Most high power femtosecond lasers suffer from “prepulses” of different origin. These prepulses can lead to the uncontrolled formation of plasmas of relatively long scale length before the actual high intensity main pulse arrives. This problem becomes severe at relativistic intensities. The development of plasma instability at $L \sim 100\text{--}200\lambda$ using femtosecond pulses has been reported in Ref. [8].

In this paper we report on the observation of the onset of a plasma parametric instability in a weakly relativistic regime in plasma with $L \approx \lambda_0$. The instability manifested itself in the emission at approximately 3/2 times the fundamental frequency ω_0 . The angular distribution and spectrum of the emitted 3/2 harmonic suggest that a hybrid instability—a combination of the two-plasmon decay instability (TPD) and

stimulated Raman scattering (SRS)—occurs. Two important features of the present study are: (i) The plasma was produced by the interaction of high-contrast-ratio femtosecond laser pulses with a solid target; (ii) the plasma scale length was changed in a controlled way in order to explicitly investigate its influence on the instability threshold.

The TPD and SRS instabilities, which are well known from experiments with nanosecond lasers [6], develop in the plasma regions with $n_e \sim n_c/4$ and $n_e \leq n_c/4$, respectively. Here n_c and n_e are the critical density for the incident radiation and the local electron density. In these processes a laser photon decays and produces either two plasmons (TPD) or a plasmon and a photon (SRS) with the frequencies ω , $\omega_0 - \omega$ and wave vectors \mathbf{k} , $\mathbf{k}_0 - \mathbf{k}$.

The 3/2 ω_0 emission is a typical characteristic of the TPD instability in inhomogeneous plasmas. The role of the SRS instability is usually negligible. The instability threshold is mostly determined by the plasma gradient scale length L and is usually much higher for SRS [6,9–11]. The 3/2 harmonic is generated as a result of a sum frequency mixing (SFM) of the plasmon with a laser photon ($\omega_{3/2} = \omega_0 + \omega$). According to the model proposed by Gusakov [12] the TPD and SFM regions are, generally speaking, separated in space. The plasmon wave vector changes as it propagates through an inhomogeneous plasma. The harmonic generation takes place in a plasma layer where the phase matching condition $\mathbf{k}_{3/2} - \mathbf{k}_0 - \mathbf{k} \approx 0$ is fulfilled.

Collisional damping and Landau damping limit the plasmon propagation length in the directions along and opposite to the plasma gradient, respectively. A different mechanism of the phase matched 3/2 harmonic emission has been discussed in Ref. [13]. In this case the phase matching condition can be fulfilled “locally” due to the additional coupling of the TPD instability to ion-acoustic waves. In experiments with nanosecond pulses the coupling to ion waves also plays an important role in nonlinear saturation of the instability [10,14].

The classical relation of the frequency shift $\Delta\omega \equiv \omega - \omega_0/2$ of the plasmon with respect to $\omega_0/2$ and its wave vector \mathbf{k} can be found from energy and momentum conservation and the dispersion relations [14,15]

$$\Delta\omega = \frac{3}{8} \omega_0 r_d^2 (2\mathbf{k}_0 \cdot \mathbf{k} - k_0^2), \quad (1)$$

where r_d is the Debye radius. Roughly speaking, the “blue”

*Electronic address: tar@iep.physik.uni-essen.de

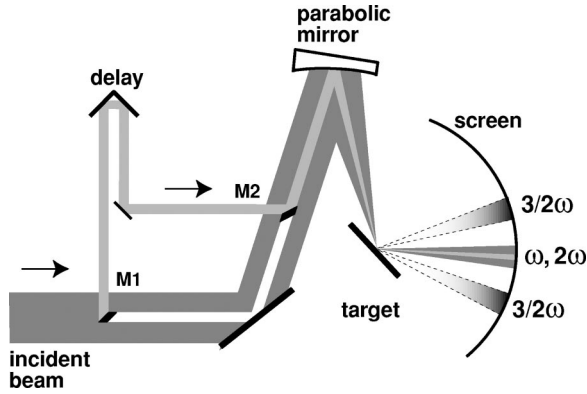


FIG. 1. Experimental schematic.

plasmon ($\Delta\omega > 0$) generated by the incident wave initially propagates *into* ($\mathbf{k}_0 \cdot \mathbf{k} > 0$) and the “red” ($\Delta\omega < 0$) one *out of* ($\mathbf{k}_0 \cdot \mathbf{k} < 0$) the plasma. Normally, the length of the plasmon wave vector significantly exceeds k_0 .

The spectrum and the angular distribution of the $3/2 \omega_0$ emission are determined by both the spectrum of the TPD and the phase matching condition. In the experiments with nanosecond pulses the spectrum typically consists of two peaks: a component that is redshifted with respect to exactly $3/2 \omega_0$ and a blueshifted peak corresponding to the “red” and “blue” plasmons [9,14–16]. The width of the peaks and the distance between them are usually a few nanometers. As a rule the intensity of the “blue” peak is lower than that of the “red” one (3–5 times). In Gusakov’s model this observation is attributed to the fact that the blue plasmon initially propagates *into* the plasma, resulting in higher overall absorption [14,16]. A somewhat more complicated spectral structure has been observed in a long wavelength experiment with a CO₂ laser [17]. Only the redshifted component of the $3/2$ harmonic spectrum was present with a total width of 150–200 nm. It consisted of a series of peaks separated by approximately 30 nm. This spectral structure was associated with the coupling of the TPD to ion-acoustic waves [13].

II. EXPERIMENT

In our experiments we used a titanium sapphire laser producing 200-mJ pulses of 120 fs duration at a wavelength of 800 nm. The ratio of the pulse peak intensity to the intensity at 1 ps (intensity contrast) was determined to be about 10^5 . The ASE intensity contrast was approximately 10^9 . A schematic representation of the experimental setup is shown in Fig. 1. The p-polarized incident laser beam was focused onto the target with the help of an off-axis parabolic mirror. The targets were optically polished glass substrates, which were raster scanned to provide a fresh surface for each laser pulse. The diameter of the “main” beam in the focal plane of the parabolic mirror was $6 \mu\text{m}$ (full width at half maximum FWHM). About 40% of the pulse energy was concentrated within this circle. The peak intensity on the target surface was $7 \times 10^{17} \text{ W/cm}^2$, corresponding to normalized laser wave amplitude $a_0 \equiv eA_0/mc^2 \approx 0.6$. The experiments were performed in a vacuum chamber at an ambient pressure of 10^{-3} Torr.

The beam providing the controlled “prepulse” was formed from the “main” beam with the help of the small mirrors M1 and M2 and an optical delay as shown in Fig. 1. The diameter and the intensity of the “prepulse” beam on the target surface were $19 \mu\text{m}$ (FWHM) and 10^{15} W/cm^2 , respectively. The time dependence of the plasma scale length $L = n_e (dn_e/dx)^{-1}$ at $n_e = n_c/4$ and the electron temperature were estimated using the “MEDUSA” hydrocode [18]. According to this estimate the electron temperature after the “prepulse” was about 200 eV.

The angular distribution of the reflected light was observed on a screen with the help of a charge-coupled device (CCD)-camera. The screen had a cylindrical shape with the axis going through the focus of the parabolic mirror (Fig. 1). The reflected radiation at the fundamental frequency was attenuated with the help of suitable optical filters.

The angular profiles of the energy distribution on the screen for the angle of incidence of 38° and different delay times are shown in Fig. 2. At short delays only the collimated beam of the reflected fundamental and second harmonic radiation in the direction of the specular reflection is present [Fig. 2(a)]. However, starting from a certain delay time green $3/2$ harmonic emission can be seen [Fig. 2(b) and 2(c)]. It is interesting that in a particular range of delay times (see below) the $3/2$ harmonic emission occurs in the form of two well-collimated beams at angles with respect to the target normal of $\sim 25^\circ$ and $\sim 75^\circ$, respectively. The two-beam emission similar to that shown in Fig. 2(b) has been observed for the angles of incidence in the range from 30° to 45° . For other angles only one collimated harmonic beam (with smaller emission angle) was present. At all possible delay times and the angles of incidence from 20° to 70° , no harmonic radiation in the backward direction was generated.

In Fig. 3 the $3/2$ harmonic energy is plotted as a function of delay time (lower horizontal scale) and scale length (upper horizontal scale). The dashed vertical lines show the range in which the $3/2$ harmonic was emitted as two collimated beams. It can be seen that the instability already develops at a very steep plasma-vacuum interface. The energies of the $3/2$ harmonic at the angles of $\sim 25^\circ$ and $\sim 75^\circ$ were approximately equal. The total energy of the $3/2 \omega_0$ emission is about $10 \mu\text{J}$ at the delay time of 30 ps ($L \approx 1.2\lambda_0$), resulting in the conversion efficiency of 5×10^{-4} [19].

The spectra of the two collimated beams of the $3/2$ harmonic were also measured separately. The calibration of the spectrometer (grating 600 l/mm, focal length 500 mm) was checked with the help of the second harmonic of the Nd:YAG (YAG, yttrium aluminum garnet) laser (532 nm) which nearly coincides with a wavelength $\lambda_{3/2}$ corresponding to exactly $3/2 \omega_0$ ($533 \pm 1 \text{ nm}$). The spectrometer calibration accuracy and resolution were $\sim 0.1 \text{ nm}$.

The harmonic spectrum has a fluctuating substructure (Fig. 4), which can be attributed to the manifestation of thermal noise from which the parametric instability starts. The characteristic width of the single peaks ($\sim 7 \text{ nm}$) in the spectrum is given by the inverse duration of the laser pulses. Unlike in the case of nanosecond pumping, much shorter pulse duration makes the spectral peaks easily resolvable in a single pulse spectrum.

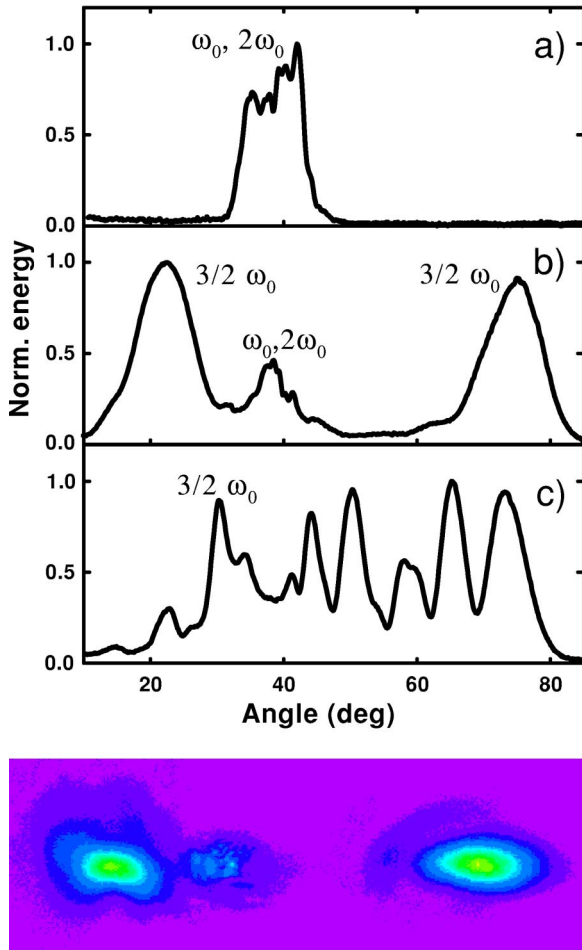


FIG. 2. (Color online) Angular distribution of the radiation emitted from the target surface for different delay times Δt : (a) $\Delta t = 2.5$ ps, $L \sim 0.3\lambda_0$; (b) $\Delta t = 25$ ps, $L \sim 1.1\lambda_0$; (c) $\Delta t = 35$ ps, $L \sim 1.4\lambda_0$. The observed structure in the profile of the specularly reflected beam ($\omega_0, 2\omega_0$) is connected with the diffraction on mirrors M1 and M2 (see Fig. 1). The profiles are recorded in a single pulse. At $\Delta t = 35$ ps the distribution strongly fluctuates from pulse to pulse. Below is the actual distribution on the screen at $\Delta t = 25$ ps, $L \sim 1.1\lambda_0$ recorded with a CCD camera.

Figure 5 represents the spectra averaged over 200 laser pulses for the angle of incidence of 38° . For the delay time of 22 ps [Fig. 5(a)] the 3/2 harmonic was generated in the form of two collimated beams (see Fig. 2). Unlike the regular spectra of the 3/2 harmonic [9,16,14,15] the observed spectra have no double-peaked structure. The spectrum of the collimated emission at the angle of 75° is centered around 533 nm. The spectrum at 25° is strongly shifted to shorter wavelengths, which is not typical for 3/2 harmonic spectra. Somewhat narrower spectra were obtained at the delay time of 40 ps [Fig. 5(b)]. For this delay time the harmonic radiation is spread over a wide solid angle. The spectra were measured at the angles of 25° and 75° with an acceptance angle smaller than 0.3 sr.

III. DISCUSSION

The important feature of femtosecond laser interaction with a steep gradient plasma is that at least at small L the

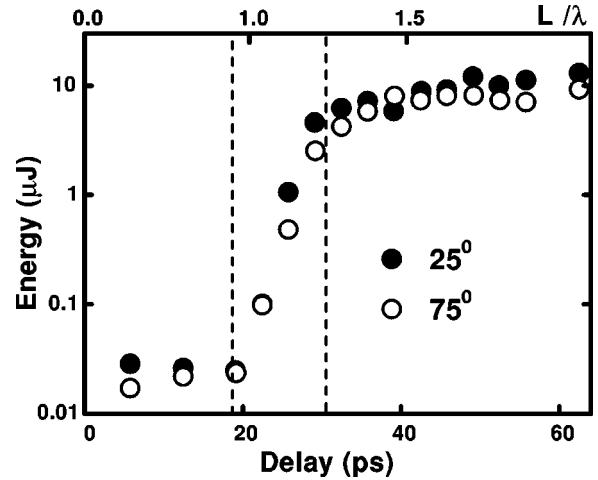


FIG. 3. Dependence of the energy of the 3/2 harmonic for the angles of 25° and 75° on the delay time and L . The energy of about 20–30 nJ at small delays corresponds to noise level. The dashed vertical lines show the range in which the 3/2 harmonic is emitted as two collimated beams.

plasma can be considered as one dimensional. Moreover, the plasma instabilities are purely electronic because during the interaction the ions have not enough time to move. The coupling of the electron plasma waves to the ion-acoustic modes [13] can be neglected. In this case the wave vectors of the plasmons responsible for the 3/2 harmonic emission can be found from the phase matching condition as shown in Fig. 6. Note that as a result of dispersion the experimental angle of incidence of 38° and the harmonic emission angle of 75° correspond to 45° and $\sim 90^\circ$, respectively, at $n \sim n_c/4$ (inside the plasma). Also, the lengths of the wave vectors at $n \sim n_c/4$ are $|\mathbf{k}_0| \approx 0.87 \omega_0/c$ and $|\mathbf{k}_{3/2}| \approx 1.4 \omega_0/c$. It can be seen that the harmonic beams at 25° and 75° are produced by plasmons propagating along the plasma gradient (\mathbf{k}_1) and those with $\mathbf{k} \approx \mathbf{k}_0$ (\mathbf{k}_2). According to Fig. 5 the spectra of the plasmons are different.

The pump intensity in our experiments could exceed the

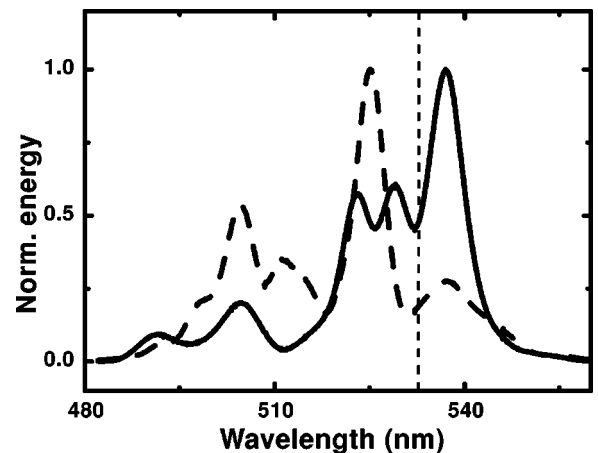


FIG. 4. Spectra of the 3/2 harmonic emitted at the angle of 25° recorded in two successive laser pulses. The delay time is 34 ps. The vertical dotted line corresponds to exactly $3/2 \omega_0$.

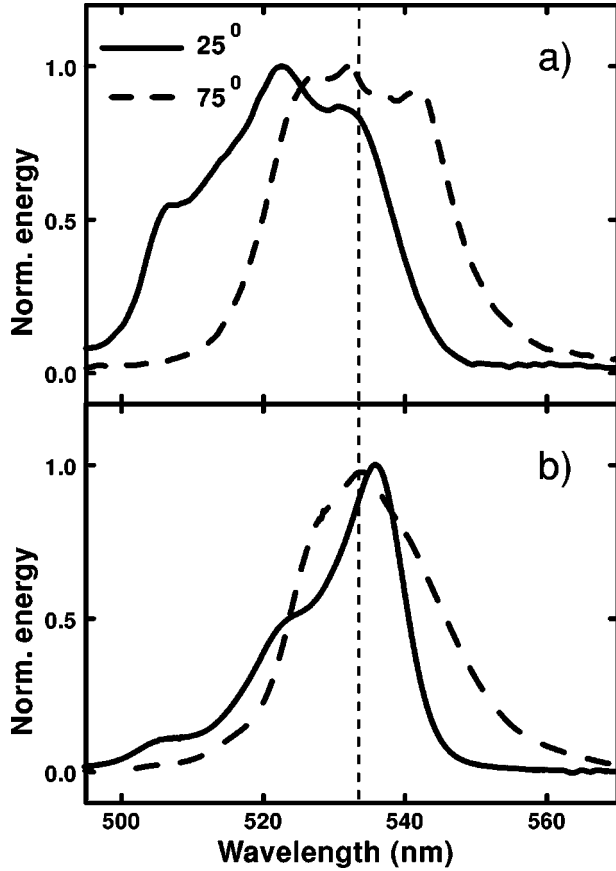


FIG. 5. Spectra of the 3/2 harmonic averaged over 200 laser pulses for the angles of 25° and 75° at $\Delta t = 22$ ps (a) and at $\Delta t = 40$ ps (b). The vertical dotted line corresponds to exactly $3/2 \omega_0$.

thresholds for both TPD and SRS instabilities at $L \sim \lambda_0$. However, the high amplification for plasmons with \mathbf{k} directed at $\sim 45^\circ$ with respect to \mathbf{k}_0 is typical of the TPD instability [6]. The plasmon with the initial wave vector of \mathbf{k}'_1

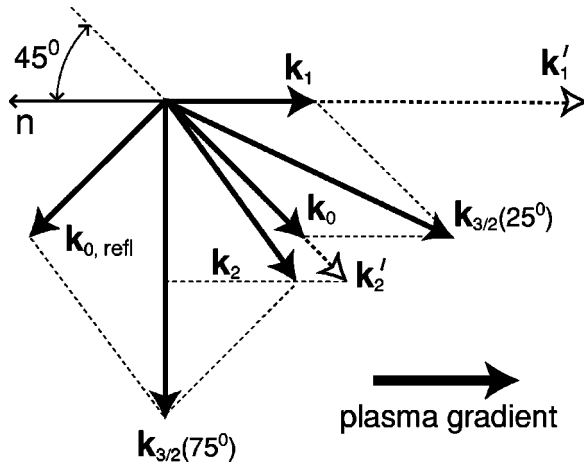


FIG. 6. SFM phase matching. \mathbf{k}_0 ($\mathbf{k}_{0,refl}$) and $\mathbf{k}_{3/2}$ are the wave vectors of the pump (reflected pump) and 3/2 harmonic waves, \mathbf{k}_1 and \mathbf{k}_2 are the plasmon wave vectors after they have reached the proper length on their way through the plasma. \mathbf{k}'_1 and \mathbf{k}'_2 correspond to the initial plasmons.

propagating along the plasma gradient rapidly changes its momentum. The “blue” plasmons initially propagating *into* the plasma decrease their \mathbf{k} vectors (Fig. 6) until the phase matching condition for SFM is reached. Due to high temperature and small L the collisional absorption is weak. This helps to meet the phase matching condition for the 3/2 harmonic generation in a wide spectral range. On the other hand, the “red” plasmon moves *out* of the plasma and $|k|$ increases. This difference in plasmon behavior could explain the blueshift in the harmonic spectrum [20].

The normalized plasmon path during the laser pulse is $l/\lambda_0 = v_g \tau / c T_0 \approx 0.5(kc/\omega_0)T[\text{keV}]$, where v_g is the plasmon group velocity, τ is the pulse duration, T_0 is the period of the pump wave, and T is the electron temperature. For a rough estimate we take the plasmon wave vector length to be $|\mathbf{k}| \sim \omega_0/c$ (the one needed for the phase matched SFM) and $T = 2$ keV. This gives $l \sim \lambda_0$. Due to the short plasma scale length $L \sim \lambda_0$ this path is enough for sufficient change of the wave vector length. The increase of L may then lead to narrower 3/2 harmonic spectra, which is consistent with our experimental observations [Fig. 5(a) and 5(b)].

The plasmon with $\mathbf{k}'_2 \approx \mathbf{k}_0$ could also be produced by TPD. Propagating *into* the plasma, according to Fig. 6, it has to change the length and the direction of its wave vector only slightly in order to satisfy the phase matching condition. The harmonic emission generated at $\sim 90^\circ$ with respect to the target normal escapes from the plasma at 75° due to dispersion. However, according to Eq. (1) the spectrum of this TPD plasmon must be blue-shifted [21]. This does not agree with the measured spectrum of the 3/2 harmonic (Fig. 5). On the contrary, the SRS plasmon with $\mathbf{k}'_2 \approx \mathbf{k}_0$ is consistent with the measured spectrum. From the photon and plasmon dispersion relations we find that the spectrum of the 3/2 harmonic corresponding to $|\mathbf{k}| \sim \omega_0/c$ is centered around $3/2 \omega_0$ for $T \sim 2$ keV. This is a reasonable temperature under our experimental conditions. Unfortunately, the equal thresholds for 3/2 harmonic generation measured for 25° and 75° emission do not agree with the fact that the threshold for the SRS instability in an inhomogeneous plasma is normally higher than the threshold for the TPD instability [10,6,9].

A possible explanation for this peculiarity is that a hybrid SRS-TPD [4,5,22,11] instability occurs. On the one hand, according to Ref. [10], for the normalized laser amplitude $a_0 \approx 0.6$ and $T \sim 2$ keV the threshold scale lengths for the SRS and the TPD instabilities differ only by a factor of about 2. On the other hand, it is clear that if $\mathbf{k} \approx \mathbf{k}_0$ the beating of the plasmon with the pump wave will produce an electromagnetic (SRS) as well as the electrostatic (TPD) response. In other words, at $\mathbf{k} \approx \mathbf{k}_0$ a combination of TPD and SRS instabilities is excited. For example, according to Ref. [4] (homogeneous plasma with $n \sim n_c/4$, normalized laser amplitude $a_0 = 0.2$), the instability growth rate assumes a maximum for two different plasma waves: (i) for $\mathbf{k} \approx (1.1 - 1.2)\mathbf{k}_0$ (hybrid plasmons) and (ii) for a wide spectrum of \mathbf{k} directed at $\sim 45^\circ$ with respect to \mathbf{k}_0 (TPD-type ones).

The measured harmonic spectra are unusually broad. Note that the relative wavelength shift $\Delta\lambda/\lambda_{3/2}$ is much bigger

than the one reported in Ref. [17]. The underlying plasmon spectrum is even broader because not all plasmons satisfy the SFM phase matching conditions mentioned above. In Fig. 5(a) the shift from the wavelength of 533 nm reaches 30 nm on the blue side. This exceeds the shift allowed by Eq. (1). Indeed, the length of the plasmon \mathbf{k} vector is limited by Landau damping so that $kr_d \lesssim 0.4$ [6]. At the same time $k_0 r_d \approx 0.08 \sqrt{T(\text{keV})}$ at $n_e = n_c/4$. Substituting this into Eq. (1), one gets $\Delta\lambda_{3/2}(\text{nm}) \approx 8.5 \sqrt{T(\text{keV})} - 0.84T(\text{keV})$. This function reaches its maximum of ~ 20 nm only at about 20 keV—a much higher temperature than one would expect under our experimental conditions.

The origin of this discrepancy is not clear. The influence of the Doppler as well as the ionization blueshifts can be neglected. The spectra of the reflected fundamental and of the second harmonic do not show comparable shifts. According to Fig. 4 the spectral broadening due to the short duration of the laser pulses is only ~ 7 nm. The saturation effects due to the interaction with the ion waves, which are typical for nanosecond laser plasma interactions, are not important on the femtosecond time scale. The big spectral width of the 3/2 harmonic emission, which corresponds to a broad instability range in \mathbf{k} space, may indicate that the influence of the Landau damping becomes weaker either because of an extremely short scale length or due to the distortions of the electron velocity distribution.

IV. CONCLUSIONS

In conclusion, we have demonstrated some features of plasma instabilities in relatively steep-gradient plasma in a weakly relativistic regime. In particular, the instability develops at extremely short plasma scale lengths, and the excited plasmons have a very broad spectrum. A highly collimated 3/2 harmonic emission can be achieved. Due to one-dimensional character of the plasma, and pure electronic nature of the instability a relatively simple explanation of the spectral and angular distribution of the harmonic emission could be given.

Our results set a limit to the plasma scale length for instability-free laser solid interaction at relativistic intensities. The instability threshold can be used as an indication of the amount of plasma expansion during the interaction. The measured conversion efficiency to the 3/2 harmonic reaches similar values as in the case of nanosecond laser pulses [9]. However, in distinction to the latter case, in our experiments collimated harmonic beams are observed.

ACKNOWLEDGMENTS

We would like to thank P. Mora and V. Silin for helpful discussions, P. Gibbon for giving us access to the “MEDUSA” hydrocode, and the Deutsche Forschungsgemeinschaft for its financial support.

-
- [1] M. Tabak, J. Hammer, M.E. Glinsky, W.L. Kruer, S.C. Wilks, J. Woodworth, E.M. Campbell, M.D. Perry, and R.J. Mason, *Phys. Plasmas* **1**, 1626 (1994).
- [2] V. Malka, S. Fritzler, E. Lefebvre, M.-M. Aleonard, F. Burgy, J.-P. Chambaret, J.-F. Chemin, K. Krushelnick, G. Malka, S.P.D. Mangles, Z. Najmudin, M. Pittman, J.-P. Rousseau, J.-N. Scheurer, B. Walton, and A.E. Dangor, *Science* **298**, 1596 (2002); X. Wang, N. Saleh, M. Krishnan, H. Wang, S. Backus, M. Murnane, H. Kapteyn, D. Umstadter, Q. Wang, and Baifei Shen, *J. Opt. Soc. Am. B* **20**, 132 (2003); D. Umstadter, *Phys. Plasmas* **8**, 1774 (2001); K. Kruschelnick, E.L. Clark, M. Zepf, J.R. Davies, F.N. Beg, A. Machacek, M.L.K. Santala, M. Tatarakis, I. Watts, P.A. Norreys, and A.E. Dangor, *ibid.* **7**, 2055 (2000); S.P. Hatchett *et al.*, *ibid.* **7**, 2076 (2000); M. Schnürer, R. Nolte, A. Rousse, G. Grillon, G. Cheriaux, M.P. Kalashnikov, P.V. Nickles, and W. Sandner, *Phys. Rev. E* **61**, 4394 (2000).
- [3] A. Tarasevitch, A. Orisch, Ph. Balcou, U. Teubner, D. Klopfel, W. Theobald, and D. von der Linde, *Phys. Rev. A* **62**, 023816 (2000).
- [4] B. Quesnel, P. Mora, J.C. Adam, A. Heron, and G. Laval, *Phys. Plasmas* **4**, 3358 (1997).
- [5] H.C. Barr, P. Mason, and D.M. Parr, *Phys. Plasmas* **7**, 2604 (2000).
- [6] W. L. Kruer, *The Physics of Laser Plasma Interactions* (Addison-Wesley, Redwood City, CA, 1988).
- [7] E.Z. Gusakov, A.D. Piliya, and V.I. Fedorov, *Fiz. Plazmy* **3**, 1328 (1977) [*Sov. J. Plasma Phys.* **3**, 739 (1977)].
- [8] L. Veisz, W. Theobald, T. Feurer, H. Schillinger, P. Gibbon, R. Sauerbrey, and M.S. Jovanovic, *Phys. Plasmas* **9**, 3197 (2002).
- [9] N. G. Basov, Yu. A. Zakharenkov, N. N. Zorev, G. V. Sklizkov, A. A. Rupasov, and A. S. Shikanov, *Heating and Compression of Thermonuclear Targets by Laser Beam* (Cambridge University Press, Cambridge, 1986); N.G. Basov, V.Yu. Bychenkov, A.A. Zozulya, M.O. Kochevoi, M.V. Osipov, A.A. Rupasov, V.P. Silin, G.V. Sklizkov, V.T. Tikhonchuk, D.V. Shanditsev, and A.S. Shikanov, *Zh. Eksp. Teor. Fiz.* **92**, 1700 (1987) [*Sov. Phys. JETP* **65**, 954 (1987)].
- [10] H.A. Baldis and C.J. Walsh, *Phys. Fluids* **26**, 1364 (1983).
- [11] W. Seka, B.B. Afeyan, R. Boni, L.M. Goldman, R.W. Short, and K. Tanaka, *Phys. Fluids* **28**, 2570 (1985).
- [12] E.Z. Gusakov, *Pis'ma Zh. Tekh. Fiz.* **3**, 1219 (1977) [*Sov. Tech. Phys. Lett.* **3**, 504 (1977)].
- [13] J. Meyer, *Phys. Fluids B* **4**, 2934 (1992).
- [14] D.A. Russell and D.F. DuBois, *Phys. Rev. Lett.* **86**, 428 (2001).
- [15] A.A. Zozulya and V.P. Silin, *Fiz. Plazmy* **8**, 859 (1982) [*Sov. J. Plasma Phys.* **8**, 488 (1982)].
- [16] P.E. Young, B.F. Lasinski, W.L. Kruer, E.A. Williams, K.G. Estabrook, E.M. Campbell, R.P. Drake, and H.A. Baldis, *Phys. Rev. Lett.* **61**, 2766 (1988).
- [17] D.M. Villeneuve, H.A. Baldis, and C.J. Walsh, *Phys. Fluids* **28**, 1454 (1985).
- [18] J. Christiansen, D. Ashby, and K. Roberts, *Comput. Phys. Commun.* **7**, 271 (1974); P. A. Rodgers, A. M. Rogoyski, and S. J. Rose, RAL-89-127, 1989.
- [19] In this measurement the acceptance solid angle was about 0.3 sr. At longer delays the emission was spread over a large solid

angle and collection of the 3/2 harmonic radiation was incomplete.

- [20] The TPD plasmons propagating along the plasma surface (angle with respect to \mathbf{k}_0 also 45°) are efficiently amplified too. However, in analogy with the “red” plasmons they do not satisfy the phase matching condition.
- [21] According to Eq. (1) the wavelength shift around 533 nm at

$T=2$ keV should amount to ~ 3 nm. Taking into account the broadening due to the short pulse duration (~ 7 nm as given by the spectral width of the peaks in Fig. 4) we conclude that the “red” tail of the plasmon should not exceed a few nanometers.

- [22] B.B. Afeyan and E.A. Williams, Phys. Rev. Lett. **75**, 4218 (1995).